IN-SITU STRESS IN SHALLOW CRUST AFTER THE 2011 TOHOKU-Oki EARTHQUAKE

Taro KOYANO

1. INTRODUCTION

Crustal stress is an important factor in various fields including rock dynamics and rock engineering. They are geology, geophysics, and so on. Today, social request for assessing crustal stress field is becoming increasingly higher in fields of such as disposal of high-level nuclear wastes and storage of CO_2. And above all, the 2011 Tohoku-Oki earthquake have focused renewed attention to feasibility of earthquake forecast.

The 2011 Tohoku-Oki earthquake was the largest earthquake in recorded history in Japan which had Mw 9.0. By the earthquake, a crustal displacement of up to 5.4 m in horizontal direction and 1.2 m in vertical direction was observed in Tohoku district. It would appear that stress field in Tohoku district was greatly disturbed by such crustal movement. Therefore, in-situ rock stress measurement holds promise for application to earthquake forecast. In addition, clarifying the mechanism of change in rock stress field which affected by the earthquake promises contribution to the engineering discipline. Therefore, the aim of this study is to discuss about the relation between the earthquake and stress field in shallow crust: about few hundred meters below ground, based on in-situ rock stress measurement results after the 2011 Tohoku-Oki earthquake. In this study, in-situ stress measurement was conducted twice at the Kamaishi mine in Iwate prefecture.

2. MEASUREMENT METHOD

The compact conical-ended borehole overcoring technique (CCBO) [1] was chosen as measurement method because there are some past measurement results by this method in the Kamaishi mine. The CCBO technique is one of the stress relief methods. The CCBO technique is a suggested method [2] of International Society for Rock Mechanics (ISRM) and a standard (JGS3751-2009) [3] of Japanese Geotechnical Society (JGS). In this study, the 24-elements CCBO technique was used.

3. MEASUREMENT SITE

The Kamaishi mine where in-situ measurements were conducted is located around 170 km away from the epicenter. Crustal displacement associated with the earthquake of this district was reported to be 3.3 m in horizontal direction and 0.5 m in vertical direction. In The Kamaishi mine, there are some reliable past results obtained by the CCBO technique before the 2011 earthquake. In this study, I chose the site about 5 km back from the entrance of the 550 m level driftway as measurement site because previous measurements were conducted near the site and the site seems not to be affected by driftway and excavation. Fig. 1 is plane view of the 550 m level driftway of the Kamaishi mine. Measurement sites of past measurement results and those of this study are shown in Fig. 1. K-1 to K-5 in Fig. 1 are sites of measurements conducted by each following researchers, Sakaguchi et al. [4], Japan Nuclear Cycle Development Institute (JNC) [5], Sugawara et al., also Sugawara et al. [2] [6] and Sakaguchi et al. (using the Downward CCBO (DCCBO) technique) [7]. In this study, in-situ measurements were conducted at same site to K-5 in periods between February 27 and March 1 2012 (about 1 year after the earthquake, in borehole SKO-01), and December 17 and 19 2012 (about 2 years after the earthquake, in borehole SKO-02).

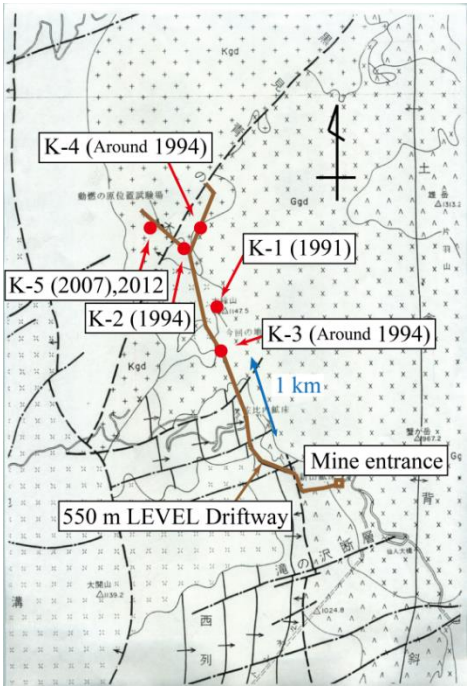

Fig. 1 Plane view of the 550 m level driftway of The Kamaishi mine.

Fig. 2 is plane view of measurement site. The borehole for the stress measurement has been drilled normal to the lateral wall of the rectangular gallery, 7 m high by 5.5 m wide, at the depth of 290 m. Therefore, assuming weight per unit volume of on-site rock is 27 kN/m^3, overburden pressure of this site is estimated 7.7 MPa. Measurements were conducted in two boreholes SKO-01 and SKO-02 showed in Fig. 2. In borehole SKO-01, measurements were conducted at following five depths from the gallery wall, 20.06 m (OC1-01), 23.57 m (OC2-01), 27.57 m (OC3-01), 28.06 m (OC4-01) and 28.56 m (OC5-01). Meanwhile, in borehole SKO-02, measurements were conducted at following three depths from the gallery wall, 27.10 m (OC1-02), 27.60 m (OC2-02) and 28.03 m (OC3-02).

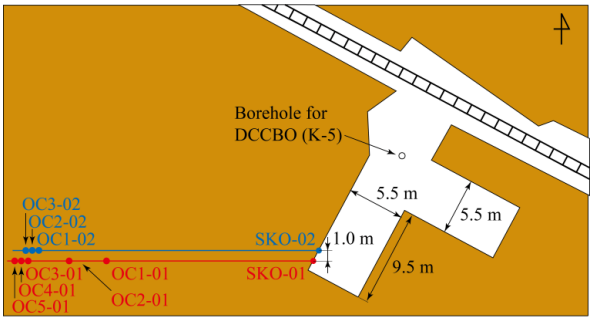

Fig. 2 Plane view of the measurement site.

4. RESULTS OF STRESS MEASUREMENT

As the result of in-situ measurements, all of strains associated with stress relief showed ideal behavior. However, the results at measurement points OC1-01, OC2-01 and OC5-01 were excluded from discussion considering the possibility that those results were affected by driftways or insufficiency of forming of borehole bottom.

Fig. 3 (a) and (b) show strains obtained at measurement points OC3-01 and OC2-02 as examples. As Fig. 3 (a) shows, up to about 2500 $\times 10^{-6}$ strain was observed in the measurement conducted 1 year after the earthquake. This value is much higher than that expected from past results. In contrast, as Fig. 3 (b) shows, despite that two measurement points are very close, strains observed in the measurement conducted 2 years after the earthquake were less than that observed in the measurement conducted 2 years after the earthquake.

After in-situ measurement, the repeating uniaxial tests on cylindrical specimens bored from recovered cores were conducted in a laboratory to determine Young's moduli and Poisson's ratios at the measurement points. As the results of the repeating uniaxial tests, all of those

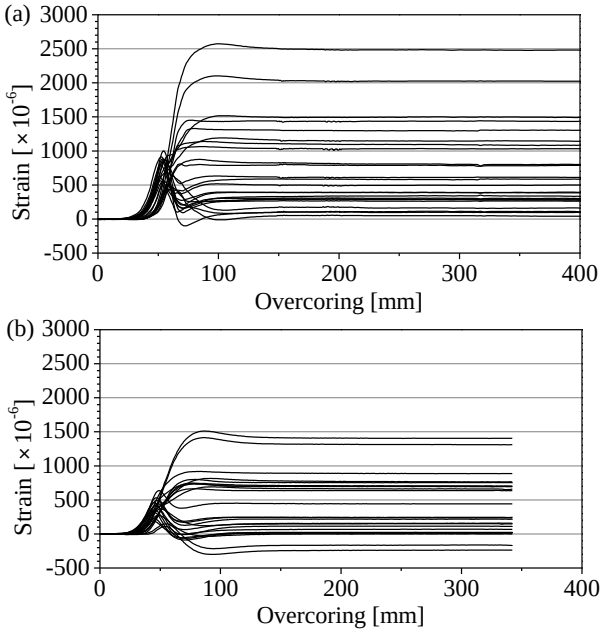

Fig. 3 Examples of strains obtained at measurement point (a) OC3-01 and (b) OC2-02.

elastic constants did not show distinguished anisotropy. Thus, average elastic constants were used for calculation of in-situ stress. Average elastic constants at each measurement points are shown in Table 1. They were in the same range of those of the past measurements.

Directions of in-situ principal stresses (σ_1, σ_2, σ_3) obtained by the past measurements, the measurement conducted 1 year after the earthquake and 2 years after the earthquake are shown in each following figures, Fig. 4 (a), Fig. 4 (b) and Fig. 4 (c). Values of in-situ principal stresses obtained by each measurement are also shown in Table 2 (a), Table 2 (b) and Table 2 (c). In addition, vertical stresses (σ_v) and overburden pressures where weight per unit volume of on-site rock is 27 kN/m^3 are also shown in Table 2 (a) to (c).

Among the direction of maximum principal stress, both of the result obtained before and after the earthquake has a general trend of compression in North-South direction. Looking in more detail, the direction of maximum

Table 1 Average Young's moduli and Poisson's ratios at each measurement point.

Measurement point	Young's modulus GPa	Poisson's ratio
OC3-01	51.5	0.21
OC4-01	57.2	0.20
OC1-02	52.8	0.16
OC2-02	57.2	0.17
OC3-02	55.9	0.17

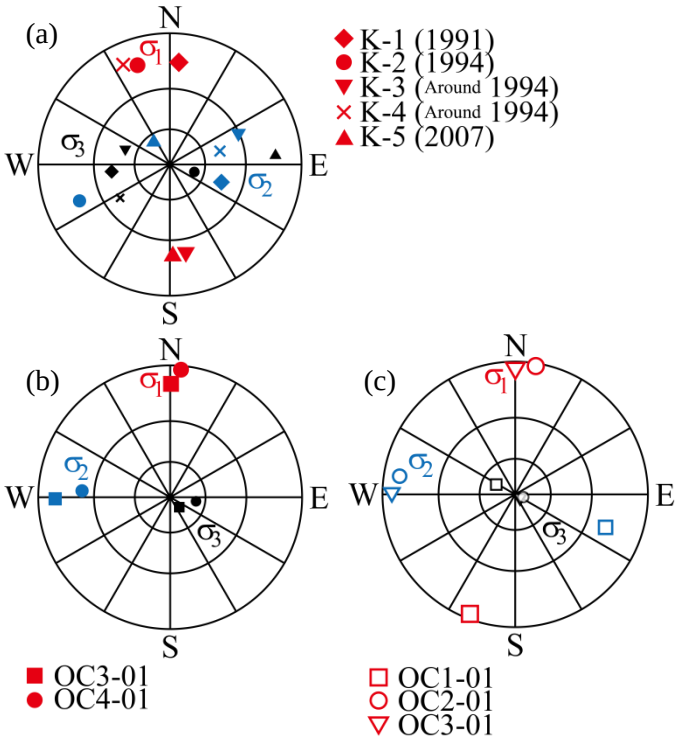

Fig. 4 Directions of in-situ principal stresses obtained by (a) the past measurement, (b) the measurement conducted 1 year after the earthquake and (c) 2 years after the earthquake.

Table 2 Values of in-situ principal stresses obtained by (a) the past measurement, (b) the measurement conducted 1 year after the earthquake and (c) 2 years after the earthquake.

(a)

Measurement point	σ_1 MPa	σ_2 MPa	σ_3 MPa	σ_v MPa	Overburden pressure MPa
K-1	22.3	14.2	4.4	10.3	13.9
K-2	29.3	7.6	2.9	4.6	7.0
K-3	27.0	7.6	6.2	8.9	11.5
K-4	25.0	8.0	6.6	7.9	6.4
K-5	10.8	7.5	2.7	7.9	7.3

(b)

Measurement point	σ_1 MPa	σ_2 MPa	σ_3 MPa	σ_v MPa	Overburden pressure MPa
OC3-01	48.2	28.4	16.3	17.2	7.7
OC4-01	43.9	31.4	17.3	19.4	

(c)

Measurement point	σ_1 MPa	σ_2 MPa	σ_3 MPa	σ_v MPa	Overburden pressure MPa
OC1-02	30.9	10.9	7.5	7.9	7.7
OC2-02	32.4	12.8	6.7	6.8	
OC3-02	31.8	12.6	3.8	4.0	

principal stress seems to have turned around from westerly direction to easterly direction. Meanwhile, directions of intermediate and minimum principal stresses changed to stress field type of reverse fault after the earthquake.

Values of in-situ principal stresses before and after the earthquake are completely different. As shown in Table 2 (b), all of values of in-situ principal stresses obtained by the measurement conducted 1 year after the earthquake are two to four times as large as those obtained by the past measurements. In addition, values of vertical stresses are 2.2 to 2.5 times as large as overburden pressure. On the other hand, as shown in Table 2 (c), while values of maximum and intermediate principal stresses are still larger than those obtained by the past measurements, they had decreased from 1 year after the earthquake. Unlike the results obtained 1 year after the earthquake, values of vertical stresses are same level to overburden pressure.

5. DISCUSSION ABOUT THE RELATION BETWEEN THE EARTHQUAKE AND STRESS FIELD

Fig. 5 shows distribution of horizontal strain after the earthquake estimated from observed data by GPS [8]. As Fig. 5 shows, Kamaishi district is in compressive strain field in North-South direction. The reason of that value of maximum principal stress increased is assumed to be due to that compressive strain in North-South direction overlapped with compressive stress field in North-South direction that already existed.

Fig. 6 shows time variation of vertical displacement observed at benchmark in Kamaishi city after the earthquake [9]. At this benchmark, vertical displacement shifted to upheaval around October 2011 after half a year of subsidence. The upheaval rate is high especially in the period between January and May 2012. The measurement 1 year after the earthquake was conducted in this period. On the other hand, the upheaval rate is quite low or nearly zero in the period between

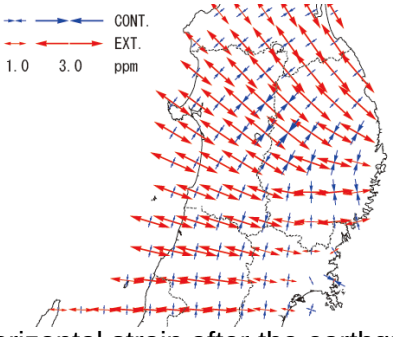

Fig. 5 Horizontal strain after the earthquake.

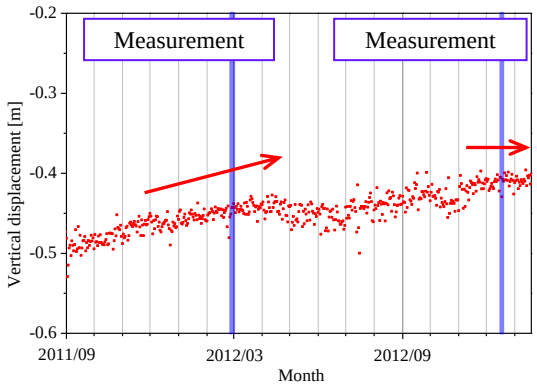

Fig. 6 Vertical displacement observed at benchmark in Kamaishi city after the earthquake.

November 2012 and January 2013 which the measurement 2 years after the earthquake was conducted in. Therefore, there is a possibility of that change of vertical stress like 2.2 to 2.5 times of the overburden pressure at the measurement 1 year after the earthquake or similar to the overburden pressure at the measurement 2 years after the earthquake is associated with the upheaval rate.

Fig. 7 shows time variation of the ratio of shear stress to average stress in the horizontal plane, $\mu m = (S_{Hmax} - S_{hmin})/(S_{Hmax} + S_{hmin})$. Before the earthquake, μm was on the increase until the measurement time of 2007 which provided the μm value of 0.56. Then μm decreased to the value at the measurement time of February 2012, and shifted to increase again. Although it is not clear how the trend of the μm value was in the period between 2007 and 2012, there is a possibility of that the μm value continued to increase until the event of the earthquake. In other words, there is a possibility of that the earthquake occurred when the μm value reached threshold of some kind.

Fig. 8 shows time variation of the direction of maximum horizontal stress. Solid curve and dotted curve in Fig. 10 are fitted curves which has a period of

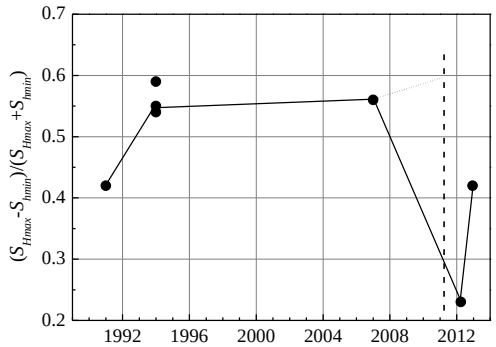

Fig. 7 Time variation of the ratio of shear stress to the average stress in the horizontal plane.

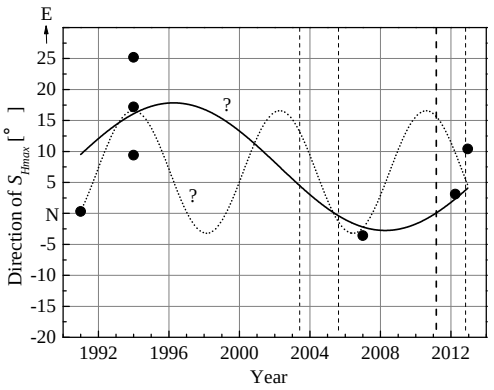

Fig. 8 Time variation of the direction of maximum horizontal stress.

24 and 8 years. Dashed lines show the events of the magnitude more than 7.0 earthquakes originating in off the coast of Miyagi prefecture. Among the solid curve, four earthquakes in Fig. 8 seem to occur in the range, shown as "Critical zone" in Fig. 8, where maximum horizontal stress assumes direction ±5 degrees around North.

6. CONCLUSIONS

As the result of in-situ stress measurements aimed at discussing about the relation between the earthquake and stress field in shallow crust, great change in the stress field in shallow crust became clear. This change seems to have some relations to the earthquake. This result suggests a benefit for the earthquake forecast from in-situ stress measurement in shallow crust. In addition, because great change in the stress field was obtained in shallow crust, the need of planning and construction control considering the effects on the stress field by the earthquakes was suggested.

REFERENCES

[1] K. Sakaguchi et al., (1994). Journal of MMIJ, 110, 331-336.
[2] K. Sugawara and Y. Obara, (1999). Int. J. Rock Mech. and Min. Sci., 36, 307–322.
[3] JGS, (2009). Standard of JGS, JGS3751-2009.
[4] K. Sakaguchi et al., (1995). Journal of MMIJ, 111, 283-288.
[5] JNC, (1999). JNC TN7410 99-001.
[6] K. Sugawara and Y. Obara, (1996). Summaries of defenses at MMIJ (Sendai), 1128-1133.
[7] K. Sakaguchi et al., (2010). Journal of MMIJ, 126, 418-424.
[8] Geospatial Information Authority of Japan (GIAJ), (2011). Newsletter of Coordinating Committee for Earthquake Prediction, 87, 14-26.
[9] GIAJ, (2013). http://mekira.gsi.go.jp/index.html